Nucleobindin-2 enhances the epithelial-mesenchymal transition in renal cell carcinoma

RAN TAO[1,2], WEN-BIN NIU[3], PENG-HUI DOU[4], SHAO-BIN NI[1], YI-PENG YU[1], LI-CHENG CAI[1], XIN-YUAN WANG[1], SHU-YI LI[5], CHENG ZHANG[1*] and ZHEN-GUO LUO[4*]

[1]Department of Urology, The First Affiliated Hospital of Harbin Medical University, Harbin, Heilongjiang 150001; [2]Department of Urology, Shenzhen Luohu People's Hospital; [3]Department of Urology, Shenzhen Samii Medical Center, Shenzhen, Guangdong 518000; [4]Department of Urology, The First Affiliated Hospital of Jiamusi University, Jiamusi, Heilongjiang 154001, P.R. China; [5]Department of Pharmacy, University of California, San Diego, CA 92121, USA

Received December 3, 2018; Accepted September 13, 2019

DOI: 10.3892/ol.2020.11526

Abstract. Nucleobindin 2 (NUCB-2) is a multifunctional protein that contains several functional domains and is associated with a wide variety of biological processes, such as food intake and energy homeostasis. NUCB-2 has been demonstrated to be associated with worse malignant outcomes and cell migration in breast and prostate cancer. However, to the best of our knowledge, its clinical and biological significance in renal cell carcinoma remains unknown. In the present study, tissue specimens from 68 patients with renal cell carcinoma and 10 normal controls were collected for NUCB-2 mRNA and protein assays. The NUCB-2 level in the patients with renal cell cancer was significantly increased compared with the normal control patients. NUCB-2-knockout in the renal cancer cell line SK-RC-52 inhibited migration and invasion. In addition, the expression levels of molecules associated with epithelial-mesenchymal transition (EMT), including E-cadherin, β-catenin, Slug and Twist, were affected by NUCB-2 suppression and the zinc finger E-box binding to homeobox 1 (ZEB1)-dependent pathway. The AMP-dependent protein kinase (AMPK)/target of rapamycin complex (mTORC) 1 signaling pathway participates in the regulation of NUCB-2-mediated metastasis and EMT. Suppression of NUCB-2 also inhibited tumor nodule formation in a murine renal cell carcinoma tumor model. In summary, NUCB-2 increased migration, invasion and EMT in renal cell carcinoma cells through the AMPK/TORC1/ZEB1 pathway *in vitro* and *in vivo*.

Correspondence to: Dr Cheng Zhang, Department of Urology, The First Affiliated Hospital of Harbin Medical University, 23 Youzheng Street, Harbin, Heilongjiang 150001, P.R. China
E-mail: doctorcheng77@163.com

Dr Zhen-Guo Luo, Department of Urology, The First Affiliated Hospital of Jiamusi University, 348 Dexiang Street, Jiamusi, Heilongjiang 154001, P.R. China
E-mail: luozhenguo@163.com

*Contributed equally

Abbreviations: 4E-BP1, eIF4E-binding protein 1; ACC, acetyl-CoA carboxylase; AMPK, AMP-dependent protein kinase; EMT, epithelial-mesenchymal transition; IHC, immunohistochemistry; mTOR, mammalian target of rapamycin; mTORC, mTOR complex; NUCB-2, nucleobindin 2; RCC, renal cell carcinoma; S6K, ribosomal S6 kinases; shRNA, short hairpin RNA; ZEB1, zinc finger E-box binding to homeobox 1

Key words: nucleobindin 2, renal cell carcinoma, epithelial-mesenchymal transition, mammalian target of rapamycin complex 1, adenosine monophosphate-dependent protein kinase, zinc finger E-box-binding homeobox 1

Introduction

Renal cell carcinoma (RCC) has attracted increasing attention over the past decades (1,2), and the lack of early symptoms or signals makes timely diagnosis difficult for patients with RCC (3,4). Of the patients diagnosed with RCC, 30% present with distant metastasis following diagnosis. Once malignant metastasis occurs in patients with RCC, the 5-year survival rate is <10% (1). Due to the tendency of malignant metastasis and insensitivity to chemotherapy, the prognosis of patients with RCC is poor (5). Metastasis of malignant tumors is a complicated biological program. Malignant tumor cells migrate away from the primary tumor location, into the surrounding tissues and reach the distal organs through circulation or lymphatic channels to develop metastatic foci (6). The epithelial-mesenchymal transition (EMT) serves as an important mechanism during the metastatic process (7). EMT promotes epithelial cells to undergo dedifferentiation, resulting in a loss of polarization and fewer cell-cell junctions, whilst enhancing interstitial transformation, tumor migration and invasion (8). Zinc finger E-box binding homeobox 1 (ZEB1) is a key activator of EMT, which upregulates the plasticity of tumor cells, resulting in tumor cells displaying similar characteristics to stem cells (9). Recent studies have demonstrated that ZEB1 serves a key role in the EMT process in lung adenocarcinoma (10), colorectal cancer and breast cancer (11,12).

During the development of malignant cancer, significant metabolic disorders occur (8,13-15). Therefore, it is important

to determine whether molecules and proteins associated with energy regulation may serve as potential biomarkers for the early diagnosis of RCC. Nucleobindin-2 (NUCB-2) is a neuropeptide that serves an important role in regulating food intake and energy homeostasis (7). A number of previous reports have described NUCB-2 abnormalities in metabolic diseases (16,17), and there is considerable evidence suggesting that NUCB-2 serves an important role during the development and metastasis of breast cancer (18), prostate cancer (19-22) and colon cancer (23), and that increased NUCB-2 expression was positively correlated with metastasis of RCC and a low postoperative survival rate (24). The AMP-dependent protein kinase (AMPK)/mammalian target of rapamycin (mTOR) signaling pathway is a central pathway involved in energy metabolism and tumor development (25,26).

To the best of our knowledge, the specific role and mechanism of NUCB-2 in RCC remain unknown. In the present study, NUCB-2 expression was analyzed in the serum and tumor tissues from patients with RCC, and was correlated with metastasis and clinical pathological typing. At the cellular level, knocking out NUCB-2 reduced proliferation, migration and invasion of SK-RC-52 cells, which are derived from human RCC. Furthermore, lower NUCB-2 expression in murine kidney cancer Renca cells inhibited tumor growth and metastasis in mice.

Materials and methods

Tissue sample collection. Between October 2016 and October 2017, 68 adult patients with RCC treated at The First Hospital of Jiamusi University (Jiamusi, China) were examined. These patients included 37 men and 31 women. Patients were aged as follows: 8 patients <40 years, 40 patients between 40 and 60 years and 20 patients >60 years. Furthermore, 18, 19 and 31 patients had stage I, II and III RCC, respectively, according to the Tumor-Node-Metastasis (TNM) staging system (27). After obtaining written informed consent from patients, 10 ml blood was collected in EDTA anticoagulant tube. Serum was obtained following blood centrifugation at 1,000 x g for 15 min at 4˚C, and was stored at -80˚C for <2 months. All the 10 donors who underwent nephrectomy suffered from hydronephosis, and the intravenous pyelogram and computed tomography urography revealed that the kidneys lost function. These patients included six men and four women aged between 20 and 60 years. Tissue samples were collected after surgery and stored at -80˚C. The present study was approved by The Ethics Committee of the First Affiliated Hospital of Jiamusi University.

Human RCC cell lines. The SK-RC-1 cell line was derived from a primary clear cell RCC specimen and the SK-RC-52 cell line was derived from a clear cell RCC metastatic lesion in the mediastinum (28). Both cell lines were obtained from the Memorial Sloan-Kettering Cancer Center. The mouse renal carcinoma cell line Renca was purchased from the American Type Culture Collection. The cells were cultured in RPMI-1640 medium (Gibco; Thermo Fisher Scientific, Inc.) supplemented with 10% fetal bovine serum (Sigma-Aldrich; Merck KGaA) and 2 mM glutamine (Gibco; Thermo Fisher Scientific, Inc.) in an atmosphere of 5% CO_2 at 37˚C. Knockout of the NUCB-2 gene in SK-RC-52 cells was performed using the CRISPR-Cas9 system, and gene-editing services were provided by Beyotime Institute of Biotechnology (Haimen, China). The guide RNA sequence 5'-TCTATCTTCGCACTTTCCAC-3' targeting exon5 of NUCB -2 gene locus (NM_001352661.1) was designed by a CRISPR gRNA design tool (ATUM). ACCG was added to the 5' end of the sgRNA sense strand, and AAAC was added to the 5' end of the antisense strand to form a cohesive end to digest pGL3-U6-sgRNA-PGK-Puro with Bsa-I. The NUCB-2 knockout selected cell clones were confirmed by sequencing and the target gene expression was validated by western blotting. Cas9 nuclease was provided by Aldevron (cat. no. 9212).

Compounds and antibodies. Rapamycin, dorsomorphin and MTT were purchased from Sigma-Aldrich; Merck KGaA. SK-RC-52 cells were treated with dorsomorphin at 40 μM for 100 min at 37˚C. SK-RC-52 cells were treated or not with rapamycin at 100 nmol/l for 12 h at 37˚C. The antibodies used in the present study were purchased from EMD Millipore, BD Biosciences and Sigma-Aldrich; Merck KGaA.

Immunohistochemistry (IHC). Tissues were fixed with 10% formaldehyde for 24 h at room temperature, and tissue sections were cut into sections of 4-μm thickness and subsequently used for IHC. Tissues were blocked at room temperature for 1 h in a humidified chamber with 5% bovine serum albumin (Invitrogen; Thermo Fisher Scientific, Inc.) dissolved in PBS. Sections were incubated with a rabbit polyclonal antibody against NUCB-2 (cat. no. ab224348; Abcam; 1:100) at 4˚C overnight, and with an HRP conjugated goat anti-rabbit IgG H&L secondary antibody (cat. no. ab205718; Abcam; 1:2,000) at 37˚C for 1 h. The degree of immunostaining was semi-quantitatively evaluated blindly by two independent expert pathologists. The pathologists scored the number of positively stained cells per field in five fields under a light microscope (magnification, x200). NUCB-2 expression was calculated based on the intensity of staining and the percentage of positively stained cells. To determine the percentage of stained cells, the number of stained and unstained cells was averaged across five fields at x200 magnification.

Reverse transcription-quantitative PCR (RT-qPCR). Total RNA covering four disease stages and normal tissues from 68 patients and 10 normal donors was extracted with TRIzol® reagent (Invitrogen; Thermo Fisher Scientific, Inc.). Complementary DNA (cDNA) was reverse transcribed from the RNA using PrimeScript RT Reagent kit (Clontech Laboratories, Inc.) at 42˚C for 15 min and 85˚C for 5 sec. The sequences of the primers used were: Human NUCB-2 forward, 5'-GAGTCAACGGATTTGGTCGT-3' and reverse, 5'-TTGATTTTGGAGGGATCTCG-3' (29); mouse NUCB-2 forward, 5'-GGAGCCAAGTCCTGATCTCTAC-3' and reverse, 5'-TTCAGACAGGCCAAGGTTTT-3'; human GAPDH forward, 5'-GAGTCAACGGATTTGGTCGT-3' and reverse 5'-TTGATTTTGGAGGGATCTCG-3'; and mouse GAPDH forward, 5'-AACTTTGGCATTGTGGAAGG-3' and reverse, 5'-ACACATTGGGGGTAGGAACA-3'.

RNA was quantified by qPCR assay with Quantities SYBR Green Master mix (MedChemExpress). The PCR reactions were as follows: Stage 1, 95˚C for 15 sec; stage 2, 40 cycles

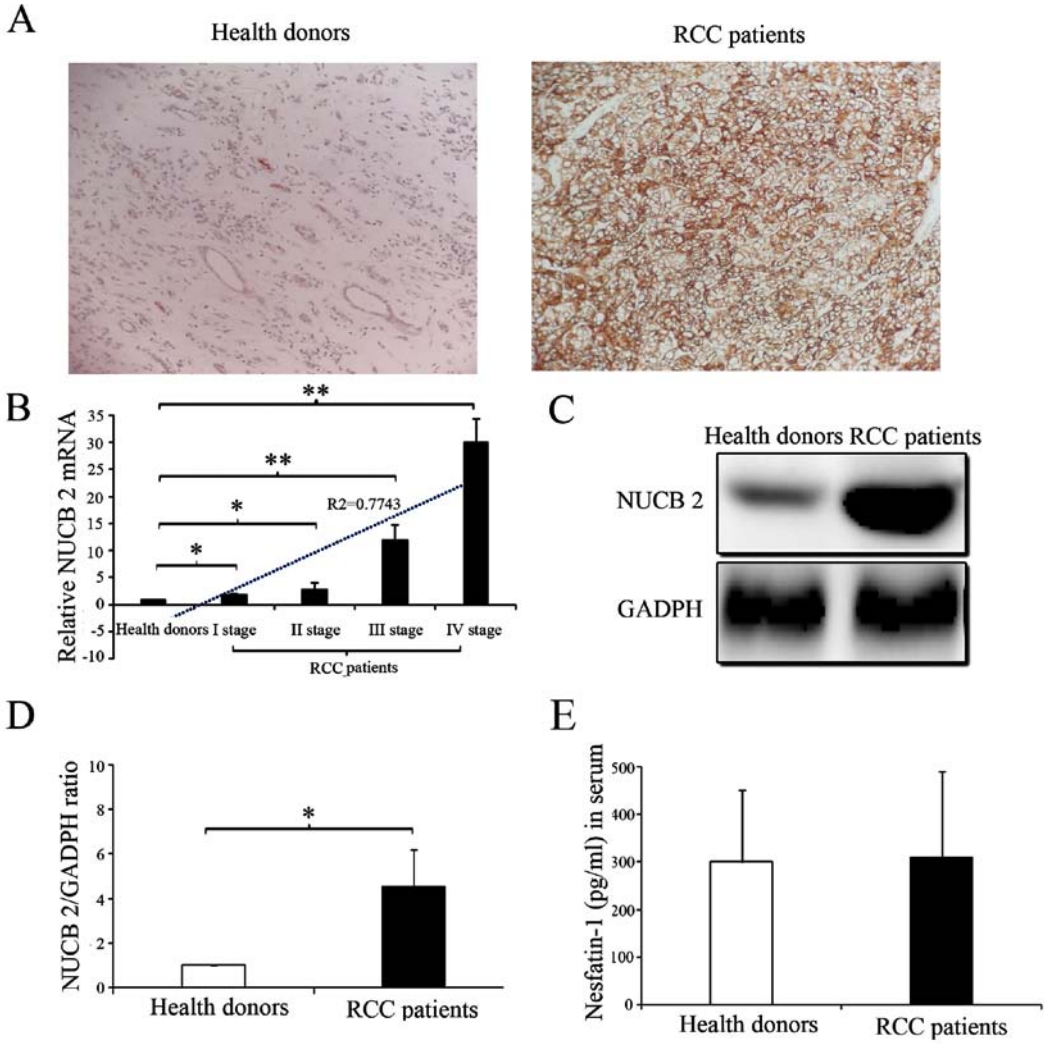

Figure 1. Expression of NUCB-2 in clinical RCC. (A) Representative example of IHC staining of NUCB-2 in a tumor tissue from a patient with RCC and a kidney tissue from a healthy donor. NUCB-2 expression was lower in the healthy donor kidney tissue compared with tumor tissue. (B) Relative mRNA levels of NUCB-2 normalized to those of GAPDH in 10 normal donors or stage I-IV CRC derived from 68 patients with RCC, including 12 stage I patients, 13 stage II patients, 25 stage III patients and 38 stage IV patients. NUCB-2 expression showed a linear increase in expression based on stage (R^2=0.7743). NUCB-2 expression was significantly increased at all stages compared with the healthy control. *P<0.05, **P<0.01. (C) Protein expression levels of NUCB-2 in patients with RCC and normal donors. (D) Densitometry analysis of the western blot shows that NUCB2 protein expression levels were significantly increased in patients with RCC compared with the healthy donors. *P<0.05. (E) Nesfatin-1 concentration in the serum of healthy donors and patients with RCC. There was no significant difference in nesfatin-1 concentration based on the presence of the disease. NUCB-2, nucleobindin 2; IHC, immunohistochemistry; RCC, renal cell carcinoma; IOD, integrated option density.

of 15 sec at 95˚C and 30 sec at 60˚C; stage 3, melting curve analysis. PCR data were analyzed using the $2^{-\Delta\Delta Cq}$ method (30) with the GAPDH gene as a control. Spearman's rank-order correlation was used for correlation analysis. The system used to grade tissues was the TNM staging system (27). The healthy donor tissue and I, II, III, IV stage tissue were ranked as 0, 1, 2, 3 and 4, respectively, and the Spearman's correlation coefficient was calculated.

Invasion and migration assays. For the cell proliferation assay, $5x10^4$ SK-RC-1, SK-RC-52 and NUCB-2-knockout SK-RC-52 cells were seeded into 96-well plates. The proliferative rate of the cells was determined with premixed WST-1 Cell Proliferation Reagent (Clontech Laboratories, Inc.) 24 h after incubation, according to the manufacturer's protocol.

A monolayer wound-healing assay was performed to compare the migratory ability of SK-RC-1, SK-RC-52 and NUCB-2-knockout SK-RC-52 cells. Cell lines were cultured until confluent, scratched and imaged using a phase-contrast microscope (magnification, x50) at 0 and 24 h. In certain experiments, MCM was added at different concentrations at the 0 h time point. The minimum distance in mm between the wound edges of the scratch area was analyzed using Adobe Photoshop version 7.0 (Adobe Systems, Inc.). All experiments were performed in triplicate.

For Transwell migration and invasion assays, a QCM™ 24-well cell migration assay and invasion system (EMD Millipore) was used. A total of $2x10^5$ cells were seeded into the inserts in 300 μl serum-free medium, and 500 μl medium supplemented with 10% FBS was placed in the lower chamber. Cells were incubated in an atmosphere of 5% CO_2 at 37˚C for 48 h. The migrated and invaded cells were stained with CyQuant GR dye (Invitrogen; Thermo Fisher Scientific, Inc.) according to the manufacturers' instructions. Migration and invasion were

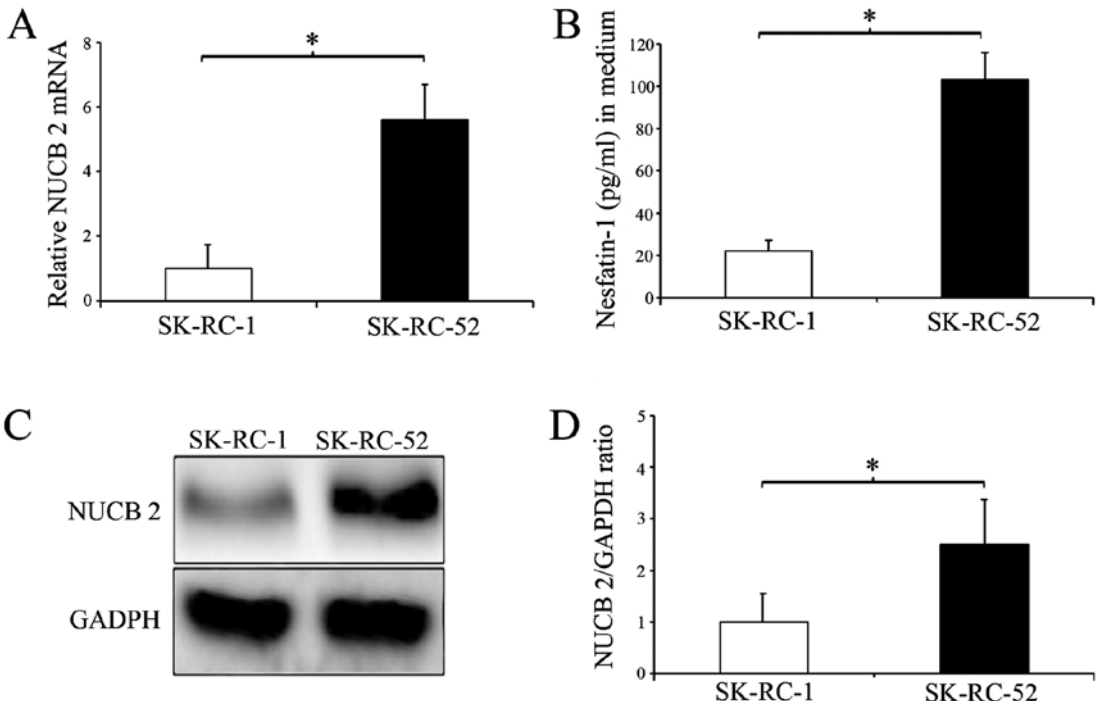

Figure 2. Expression of NUCB-2 in SK-RC-1 and SK-RC-52 cell lines. (A) Relative mRNA levels of NUCB-2 normalized to those of GAPDH in SK-RC-1 and SK-RC-52 cell lines. NUCB-2 expression was significantly higher in the SK-RC-52 cells compared with SK-RC-1 cells. *P<0.05. (B) Nesfatin-1 concentration in the cell culture medium of the two human renal cell cancer cell lines. Serum nesfatin-1 concentration was significantly higher in the SK-RC-52 cells compared with the SK-RC-1 cells. *P<0.05. (C) Protein expression of NUCB-2 in SK-RC-1 and SK-RC-52 cell lines. (D) Densitometry analysis of NUCB-2 expression relative to GAPDH. Protein concentration was significantly higher in the SK-RC-52 cells compared with the SK-RC-1 cells. *P<0.05. NUCB-2, nucleobindin 2.

assessed on a fluorometer (FLx800 Microplate Fluorescence Reader; BioTek Instruments, Inc.) using a 480/520 nm filter.

Western blotting. Cells were lysed using radioimmunoprecipitation assay buffer (EMD Millipore) on ice for 30 min. The total cell lysate was collected after centrifugation at 12,000 x g for 15 min at 4˚C. For extraction of nuclear proteins, a Nuclear Extract kit (Active Motif) was used. The concentration of protein was determined using a bicinchoninic acid protein assay kit (EMD Millipore). Proteins (50 μg) were separated by 6-12% SDS-PAGE and transferred onto polyvinylidene difluoride membranes. After transfer, 5% non-fat dry milk was used to block the membranes for 1 h. The membranes were incubated with rabbit anti-human NUCB-2 polyclonal antibody (cat. no. ab224348, 1:100, Abcam) and recombinant GAPDH antibody (cat. no. ab181602, 1:100, Abcam) at 4˚C for overnight. Membranes were washed three times in TBST for 15 min and incubated with an HRP goat anti-rabbit IgG H&L (cat. no. ab205718; 1:200; Abcam) and goat anti-mouse IgG H&L (cat. no. ab150117; 1:200; Abcam) at room temperature for 1 h. Signals were visualized using enhanced chemiluminescence substrate (EMD Millipore) on an imaging capture system (Alpha Imaging).

In vivo experiments. Short hairpin (sh)RNAs targeting human NUCB-2, mouse NUCB-2 and a control vector construct were obtained from Beyotime Institute of Biotechnology. Cells were transfected with each shRNA plasmid using Lipofectamine 2000 reagent (Invitrogen Thermo Fisher Scientific, Inc.). One day before transfection, cells were seeding at the density of $2x10^6$ cells in 10 cm dish, so that they can reach 30-50% confluence at the time of transfection. shRNA duplex (300 pmol) and Lipofectamine 2000 (Invitrogen; Thermo Fisher Scientific, Inc.; 30 μl) were added to each dish containing cells for 24 h at 37˚C in a 5% CO_2 incubator before cells were injected into mice.

All procedures were performed in an animal facility using protocols approved by The Institutional Animal Care and Use Committee of The Jiamusi University Affiliated No. 1 Hospital (Jiamusi, China). A total of 12 six-week-old male BALB/c mice weighing 18-22 g were obtained from the animal center of Jiamusi University, and housed under controlled illumination (12:12 h light/dark cycle; lights on/off, 6/18 h) and temperature (22±2˚C) for 7 days with food and water available *ad libitum*. Each group contained ten mice, and animals were injected subcutaneously into the back with 0.1 ml containing $1x10^6$ Renca cells or shRNA-Renca cells. Every other day, the size of the tumor nodules was measured. The mice were sacrificed by cervical dislocation after anesthesia when the health of the mouse continued to deteriorate and the intake of food intake continued to decrease, the weight of the mice decreased for 3 days, the mice weighed <19 grams and when the mouse tumor volume was >2,000 mm^3.

Statistical analysis. Spearman's rank-order correlation was used for correlation analysis. All data are expressed as the mean ± standard deviation. Statistical analyses were conducted using SPSS version 17.0 (SPSS, Inc.). A Student's t-test was used to compare the mean values between two experimental groups. One-way ANOVA was used to compare the mean values among three experimental groups with a least significant difference post-hoc test assuming equal variance or a Tambane's T2 post-hoc test

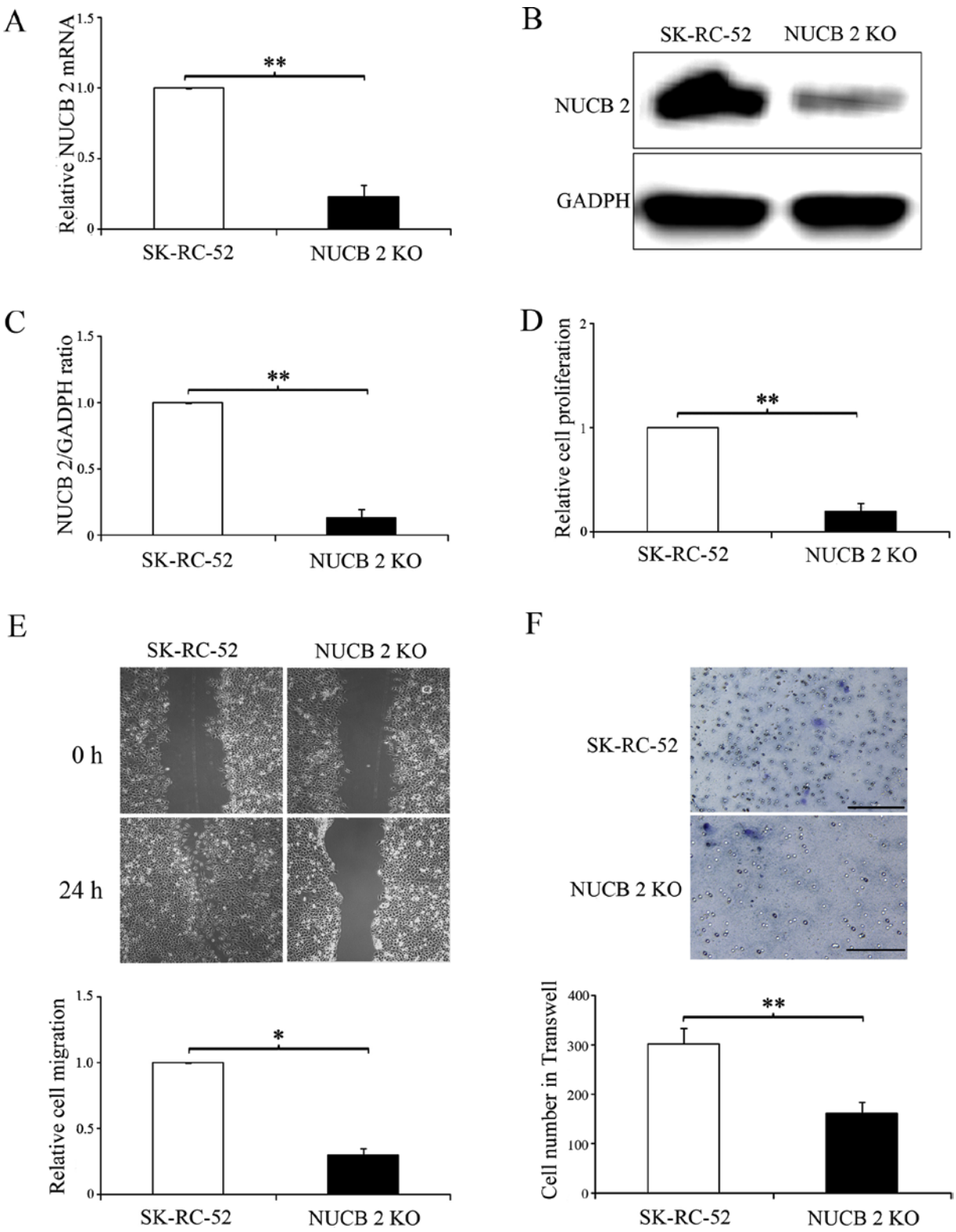

Figure 3. NUCB-2 regulates renal cell carcinoma migration and invasion. (A) Relative mRNA levels of NUCB-2 normalized to those of GAPDH in SK-RC-52 and NUCB-2-KO SK-RC-52 cell lines. NUCB-2 expression was significantly decreased in the NUCB-2-KO cells compared with the control. **P<0.01. (B) Protein expression of NUCB-2 in SK-RC-52 and NUCB-2-KO SK-RC-52 cell lines. (C) Densitometry analysis of the relative protein expression levels of NUCB-2 normalized to those of GAPDH. Protein expression was significantly decreased in the NUCB-2-KO cells compared with the control. **P<0.01. (D) Relative cell proliferation in the SK-RC-52 and NUCB-2-KO cell lines. Proliferation was significantly decreased when NUCB-2 was knocked out. **P<0.01. (E) Relative cell migration in two human renal cell cancer cell lines. Migration was significantly reduced when NUB-2 was knocked out. *P<0.05. (F) Number of cells that had migrated in the Transwell assay in two human renal cell cancer cell lines. Migration was significantly reduced when NUB-2 was knocked out. Magnification, x200. Scale bar, 200 μm. **P<0.01. NUCB-2, nucleobindin 2; KO, knockout.

when equal variance was not assumed. The adjusted significance of the P-value was set at 0.05. A population standard deviation to test the normal distribution of samples was used. P<0.05 was considered to indicate a statistically significant difference.

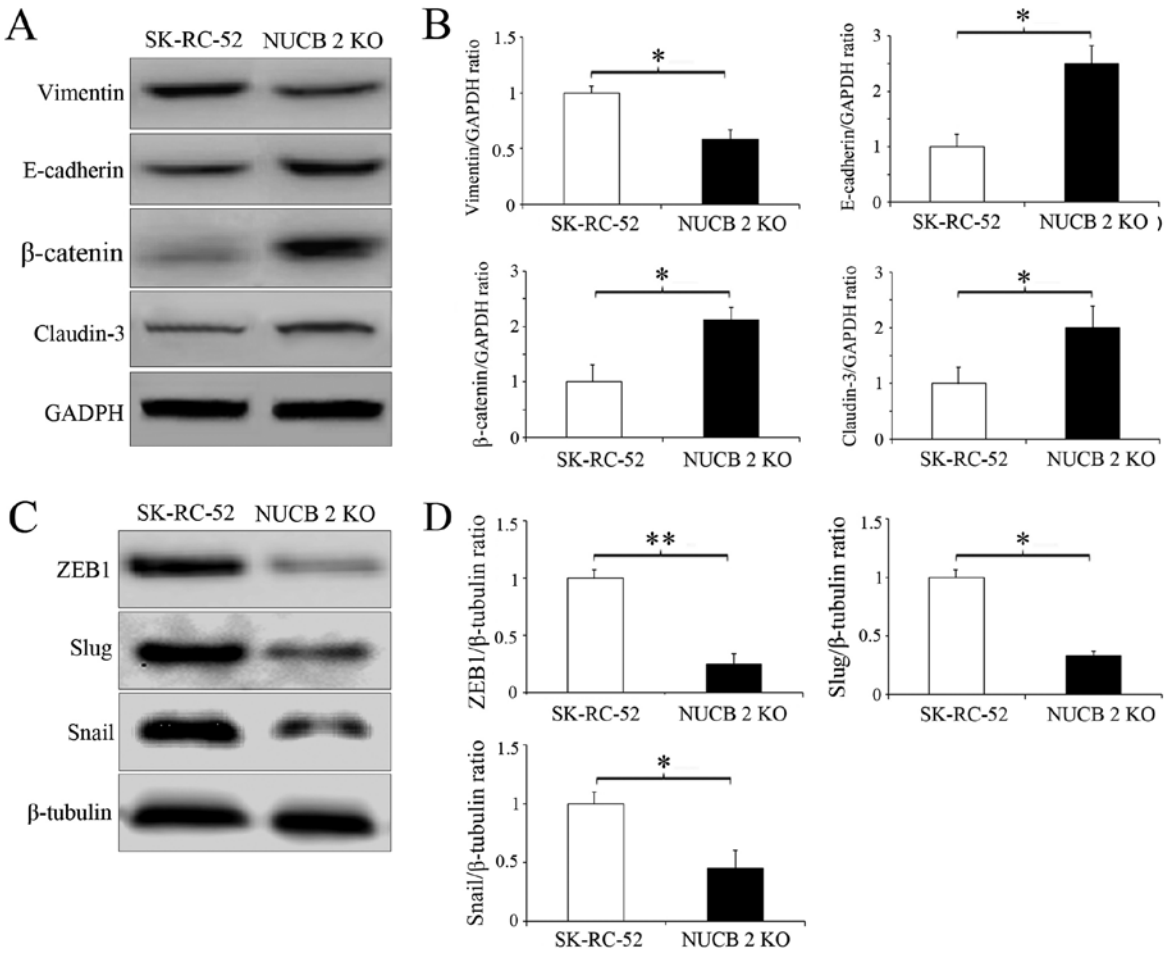

Figure 4. NUCB-2 regulates the epithelial-mesenchymal transition in renal cell carcinoma. (A) Cytosolic expression of NUCB-2, and makers of EMT, in SK-RC-52 and NUCB-2-KO SK-RC-52 cell lines. (B) Densitometry analysis of the relative protein expression levels normalized to those of GAPDH. *P<0.05. (C) Nuclear expression of NUCB-2, and markers of EMT, in SK-RC-52 and NUCB-2-KO SK-RC-52 cell lines. (D) Densitometry analysis of the relative protein expression levels normalized to those of β-tubulin. *P<0.05, **P<0.01. NUCB-2, nucleobindin 2; KO, knockout; ZEB1, zinc finger E-box binding to homeobox 1.

Results

Increased expression of NUCB-2 in RCC. The presence and distribution of NUCB-2 in the tissues were assessed via IHC. The NUCB-2 protein was primarily localized in the cytoplasm. High expression of NUCB-2 was detected in the tumor tissues of patients with RCC, whereas low expression of NUCB-2 was detected in the kidney tissues of healthy donors (Fig. 1A). The NUCB-2 mRNA and protein expression levels in the kidney tissues of 68 RCC patients and 10 normal donors were analyzed with RT-qPCR and western blot analysis. The results showed that NUCB-2 mRNA and protein expression were significantly higher in the tissue samples from patients with RCC compared with normal group (Fig. 1B-D; P<0.05). Furthermore, the expression of NUCB-2 mRNA was positively correlated with RCC stage (Fig. 1B; r^2=0.7743; P<0.05). To further determine whether NUCB-2 overexpression was systemic or local, the serum concentrations of the N-terminally active protein nesfatin-1 of NUCB-2 in both samples were determined and no significant difference was identified between the two groups (Fig. 1E).

NUCB-2 knockout reverses EMT phenotypes in RCC. In the present study, two human RCC cell lines were selected for study, SK-RC-1 and SK-RC-52 cells. These two cell lines were used to determine the effect of NUCB-2 on RCC migration and invasion, which are key steps in the initial progression of cancer metastasis (31). Higher NUCB-2 mRNA and protein expression was identified in SK-RC-52 cells compared with the SK-RC-1 cells (Fig. 2A, C and D) and higher concentrations of nesfatin-1 were identified in the cell culture medium of the SK-RC-52 cells (Fig. 2B). The SK-RC-1 cell line is derived from a primary clear cell RCC specimen, whereas the SK-RC-52 cell line is derived from a clear cell RCC metastatic lesion in the mediastinum (28); therefore, the results presented in Fig. 2 suggest that NUCB-2 may be involved in metastasis of RCC.

Based on the results of NUCB-2 expression in the two cell lines, SK-RC-52 cells were used for all subsequent experiments. The NUCB-2 gene in SK-RC-52 cells was knocked out via the CRISPR-Cas9 system, and the data demonstrated that NUCB-2 knockout was stable (Fig. 3A-C). Based on the cell proliferation (Fig. 3D), and the migration (Fig. 3E) and invasion assays (Fig. 3F), NUCB-2 knockout significantly attenuated these behaviors compared with SK-RC-52 cells. These results further demonstrate that NUCB-2 serves an important role in the metastasis of RCC.

Several biochemical markers are used to characterize EMT, for example, epithelial cells primarily express E-cadherin and

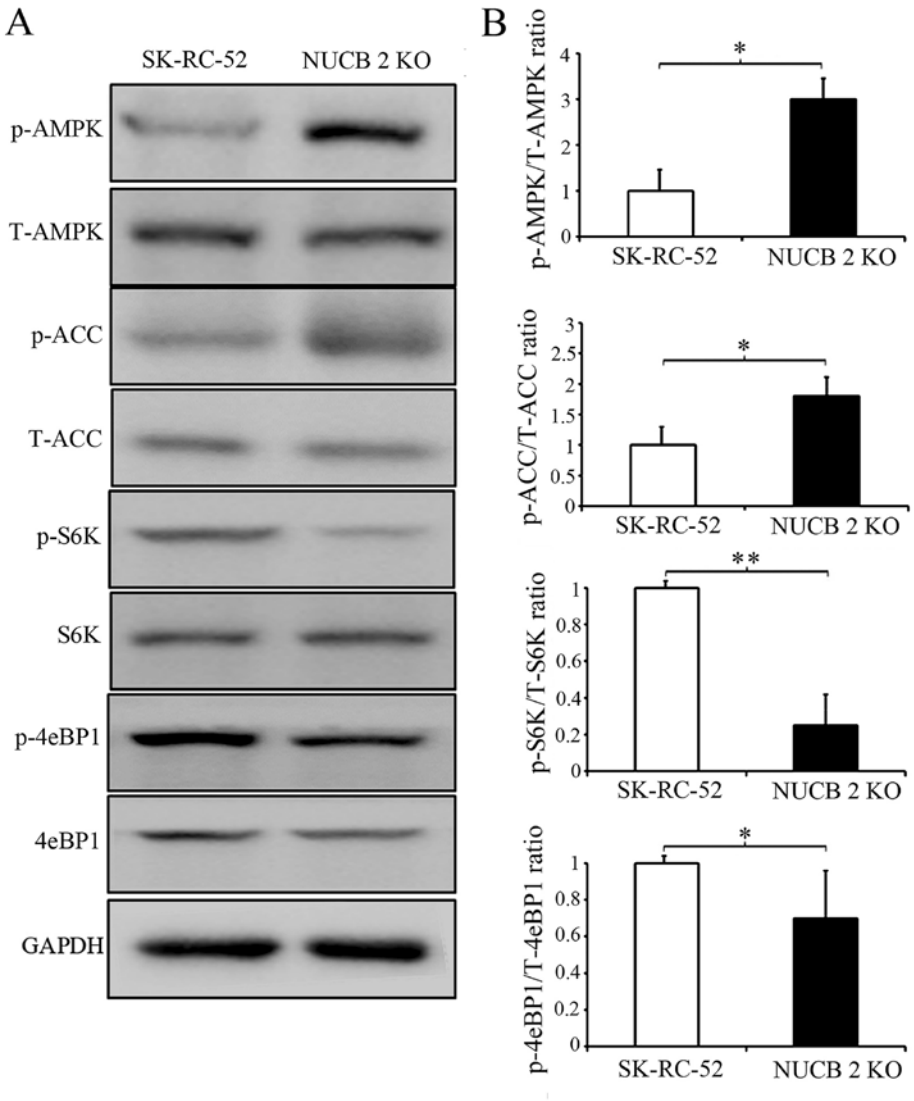

Figure 5. AMPK and TORC1 pathways are critical for regulating the NUCB-2-mediated inhibition of migration and invasion. (A) Effect of NUCB-2-KO on proteins involved in the AMPK and TORC1 pathways. (B) Densitometry analysis of the ratio of the phosphorylated variant to the total expression. Expression was first normalized to GAPDH. *P<0.05, **P<0.01. NUCB-2, nucleobindin 2; AMPK, AMP-dependent protein kinase; TORC1, target of rapamycin complex; ACC, acetyl-CoA carboxylase; S6, ribosomal S6 kinases; 4eBP1, 4E-BP1, eIF4E-binding protein 1; p-, phospho; t-, total; KO, knockout.

claudin-3, whereas mesenchymal cells express vimentin and N-cadherin (32). Since the targeted inhibition of NUCB-2 attenuated migration and invasion, it was next determined whether this inhibition was sufficient to suppress or attenuate EMT in RCC by examining the expression of the aforementioned EMT markers. The stable knockout of NUCB-2 in SK-RC-52 cells significantly increased E-cadherin and claudin-3 levels whilst significantly decreasing expression of vimentin (all P<0.05; Fig. 4A and B). ZEB1 is a major regulator of EMT in malignant tumors (32,33), and Snail and Slug are important transcription factors involved in EMT regulation (34). ZEB1 (P<0.01), Snail and Slug (both P<0.05) expression was significantly decreased in the NUCB-2-knockout cells, suggesting that NUCB-2 may be involved in EMT through the ZEB1 signaling (Fig. 4C and D).

NUCB-2 promotes EMT in RCC via the AMPK/mTOR signaling pathway. To further clarify which signaling pathway is involved in the NUCB-2-mediated EMT in RCC, the association between NUCB-2 and the AMPK/mTOR signaling pathway was assessed. Previous studies have reported that NUCB-2 affects AMPK activation and promotes mTOR phosphorylation, which leads to the upregulation of protein synthesis, cell proliferation, cell cycle progression and angiogenesis (35-37); the latter of which serves an important role in tumor metastasis. Acetyl-CoA carboxylase (ACC) is a downstream target of energy-sensitive AMPK both of which are phosphorylated in their active form. The data in Fig. 5 shows that phosphorylated AMPK and phosphorylated ACC expression was significantly increased by knocking out NUCB-2 expression in SK-RC-52 cells. These results suggest that the AMPK pathways are involved in NUCB-2-regulated EMT properties, migration and invasion in RCC. The mTOR signaling pathway is downstream of AMPK. mTOR contains two subunits of functionally and biochemically distinct multiprotein complexes called mTOR complex (mTORC)1 and mTORC2 (38-40), in which mTORC1 serves a central role in cell growth and regulation of metabolism (41).

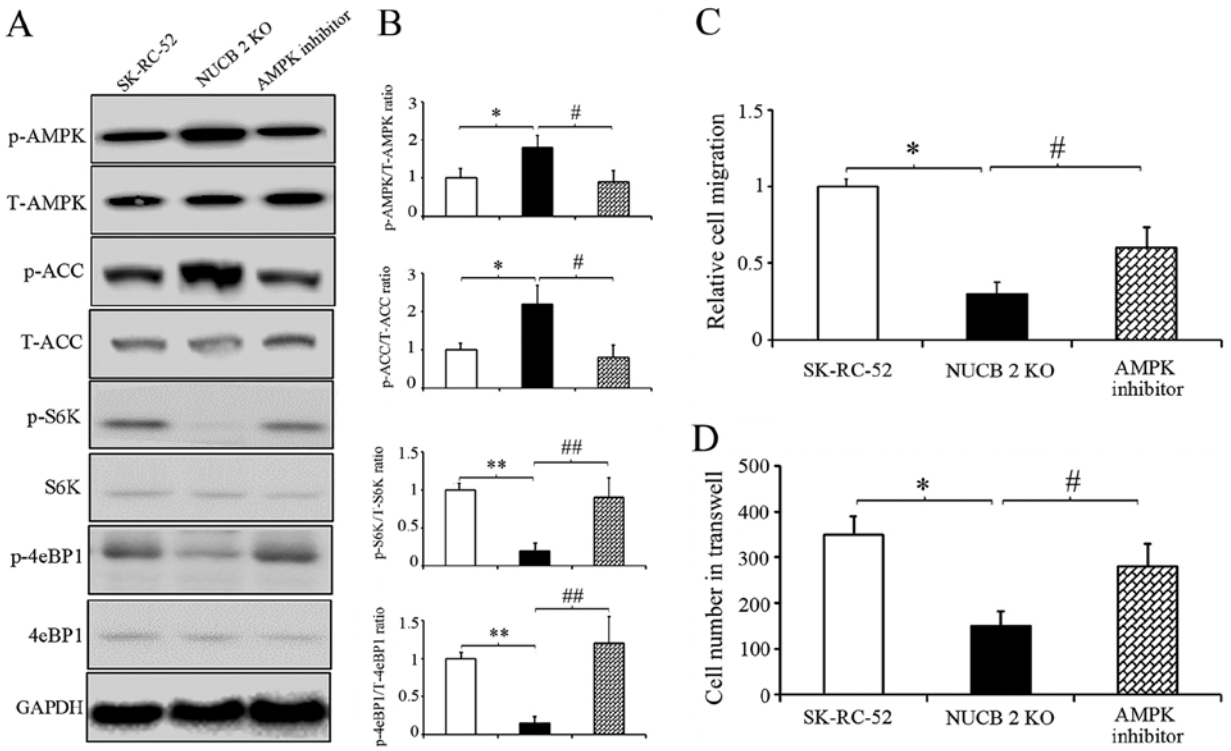

Figure 6. NUCB-2 upregulates epithelial-mesenchymal transition in renal cell carcinoma through the AMPK/TORC1 pathway. (A) SK-RC-52 cells with NUCB-2-KO were treated with 40-μM dorsomorphin or control for 100 min. (B) Effect of the inhibitor on members of the AMPK or TORC1 pathways. Densitometry analysis of the western blots in the left panel. The relative levels of protein levels normalized to those of GAPDH. *P<0.05, **P<0.01 SK-RC-52 vs. NUCB-2 KO cells; $^{\#}$P<0.05, $^{\#\#}$P<0.01 NUCB-2 KO vs. NUCB-2 KO cells treated with an AMPK inhibitor. (C) Relative cell migration in the three groups. *P<0.05, $^{\#}$P<0.05. (D) Number of invaded cells transferred in the Transwell assay in the three groups. When cells were treated with an AMPK inhibitor, the migratory and invasive abilities of NUCB-2-KO stable clones was increased. *P<0.05, $^{\#}$P<0.05. NUCB-2, nucleobindin 2; AMPK, AMP-dependent protein kinase; TORC1, target of rapamycin complex; ACC, acetyl-CoA carboxylase; S6, ribosomal S6 kinases; 4eBP1, 4E-BP1, eIF4E-binding protein 1; p-, phospho; t-, total; KO, knockout.

eIF4E-binding protein 1 (4E-BP1) and ribosomal S6 kinase (S6K) are direct substrates of mTORC1 activity (42). As shown in Fig. 5, the phosphorylation of 4E-BP1 and S6K decreased when the NUCB-2 gene was knocked out in SK-RC-52 cells, suggesting that the mTOR pathway is also involved in the NUCB-2-regulated EMT in RCC.

To further clarify the results described above, competitive AMPK inhibitor was used (43) to inhibit the AMPK signaling pathway in NUCB-2-knockout SK-RC-52 cells. After treatment with dorsomorphin (40 μM, 100 min), AMPK and ACC phosphorylation decreased, suggesting that dorsomorphin inhibition was successful. However, S6K and 4eBP1 showed the opposite results (Fig. 6A). Cell migration and invasion following treatment with dorsomorphin was also assessed. After treatment with dorsomorphin, the migratory and invasive capabilities of RCC cells were restored in the NUCB-2-knockout cells (Fig. 6B and C). Rapamycin is a commonly used TORC1 inhibitor. SK-RC-52 cells were treated without or with rapamycin (100 nmol/l) for 12 h, and EMT biomarkers were examined by western blot analysis. TORC1 inhibition resulted in significantly decreased expression of ZEB1, Snail and Slug (All P<0.01), which are involved in EMT regulation in SK-RC-52 cells, and several EMT biochemical markers experienced opposite changes (Fig. 7; P<0.01). These results suggest that NUCB-2 may promote EMT in RCC via the AMPK/mTOR signaling pathway.

In vivo experiment. To determine the role of NUCB-2 *in vivo*, the expression of NUCB-2 in the murine kidney cancer cell line Renca was inhibited by transfection with a NUCB-2-targeting shRNA (experimental group), and non-transfected Renca cells were used as a control. The results showed that the levels of NUCB-2 mRNA and protein were significantly decreased following transfection with shRNA (P<0.05; Fig. 8A-C), and tumor growth was significantly slower in the NUCB-2 inhibition group compared with the control group (Fig. 8D-G), suggesting that NUCB-2 serves an important role in RCC growth.

Discussion

The present study is the first to describe the role and mechanisms of NUCB-2 in RCC metastasis, to the best of our knowledge. NUCB-2 was highly expressed in patients with RCC, and the expression of NUCB-2 was strongly associated with clinical stage. NUCB-2 upregulated EMT through the AMPK/TORC1/ZEB1 signaling pathway. Finally, inhibition of NUCB-2 expression can inhibit the growth of RCC tumors in animals. These data suggest that NUCB-2 may be a potential marker for the diagnosis of RCC.

NUCB-2 is widely expressed throughout the body and is primarily expressed in the hypothalamic nucleus (24). NUCB-2 participates in a variety of pathophysiological processes, primarily serving an important role in maintaining

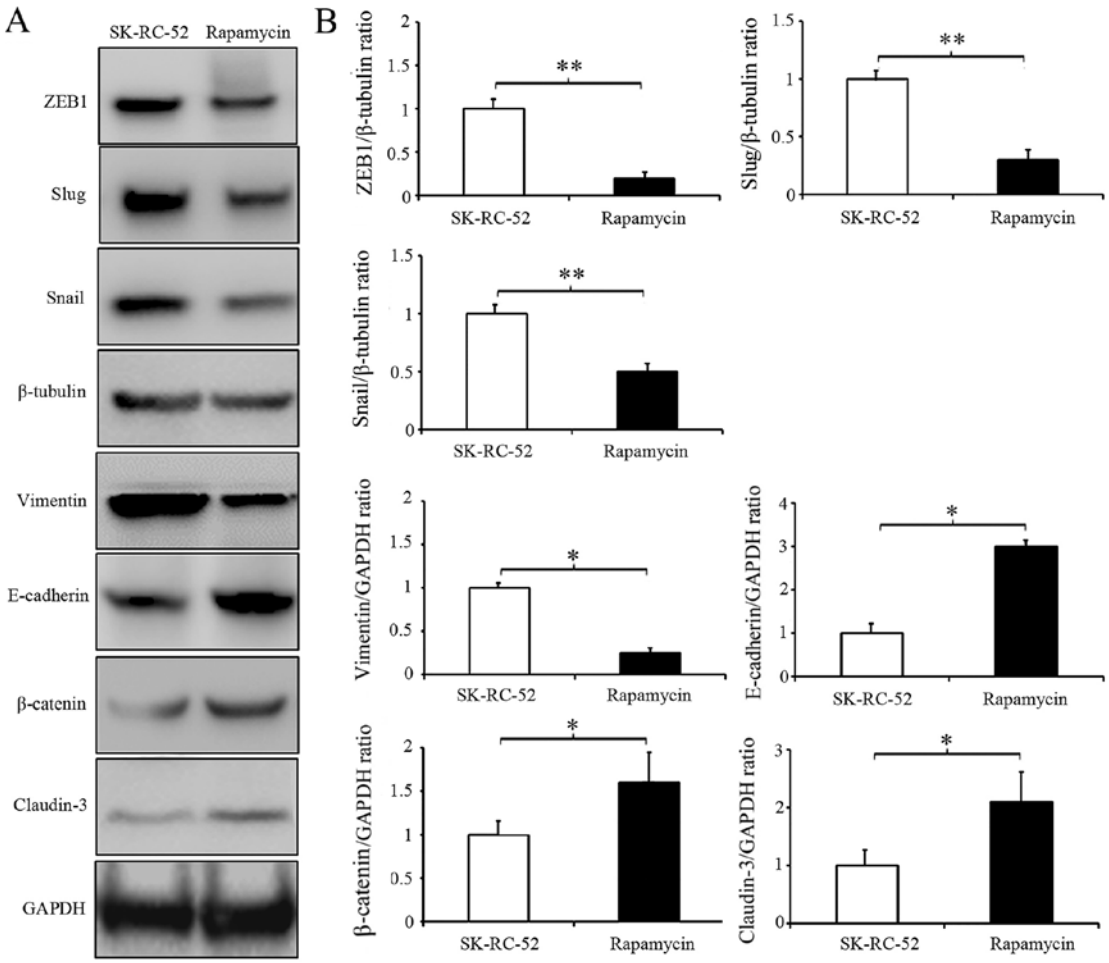

Figure 7. Rapamycin inhibits EMT in renal cell carcinoma through the TORC1/ZEB1 pathway. (A) Western blot of EMT markers in SK-RC-52 cells treated with or without rapamycin. (B) Densitometry analysis of western blots normalized to GAPDH or β-tubulin. *P<0.05, **P<0.01. EMT, epithelial-mesenchymal transition; ZEB1, zinc finger E-box binding to homeobox 1.

the energy and nutrient balance (16,17). NUCB-2 has also been demonstrated to serve an important role in tumor development. Suzuki *et al* (18) found that NUCB-2 acts as a tumor promoter during breast cancer development and metastasis. Zhang *et al* (20-22) reported that increased NUCB-2 expression is associated with prostate cancer recurrence and a poor prognosis. In a study by Qi *et al* (23), NUCB-2 was highly expressed in RCC. A retrospective clinical study by Fu *et al* (44) found that high NUCB-2 expression levels were positively correlated with Fuhrman grade. Together, these studies have concluded that NUCB-2 is associated with poor tumor prognosis. In the present study, similar results regarding NUCB-2 function in promoting RCC cell proliferation, invasion and metastasis were described. Based on the previously mentioned findings, the underlying mechanism of NUCB-2 in RCC was investigated.

The NUCB-2 gene was knocked out in SK-RC-52 cells using the CRISPR-Cas9 system and cell proliferation, invasion and migration assays were performed. The results showed that cell proliferation and metastasis were suppressed in the NUCB-2-knockout cells. EMT is a key reversible step that facilitates tumor migration, invasion and metastasis (7). Metabolic reprogramming is a distinct hallmark in EMT development (45-47). The findings of the present study implicate NUCB-2 as a key regulator of EMT in RCCs based on the observation that the increased expression of NUCB-2 in the metastatic human RCC cell line, SK-RC-52 altered expression of a number of biochemical markers (decreased E-cadherin, increased vimentin and N-cadherin). However, these markers exhibited the opposite trend in expression in SK-RC-52 cells when NUCB-2 was knocked out by genetic editing. ZEB1 is a transcription factor and a master regulator of EMT in several types of cancer (32,33). ZEB1 was highly expressed in SK-RC-52 cells, a cell line derived from RCC mediastinal metastases, suggesting that NUCB-2 may promote the malignant behaviors of RCC by upregulating ZEB1.

In various cancer cells, the activation of AMPK stimulates the tumor suppressor gene p53, which has been reported to control apoptosis and the cell cycle in the induction of the EMT and in metastasis (45-47). To investigate the mechanism underlying the high expression of NUCB-2 and renal cell proliferation and mesenchymal transition, the association between NUCB-2 and the AMPK/mTOR signaling pathways was examined. The results demonstrated that knockdown of NUCB-2 expression in SK-RC-52 cells increased the phosphorylation of AMPK and decreased mTOR phosphorylation, consistent with numerous previous studies (48-50). ZEB1, is a major mediator of tumor migration, and exerts its effects by

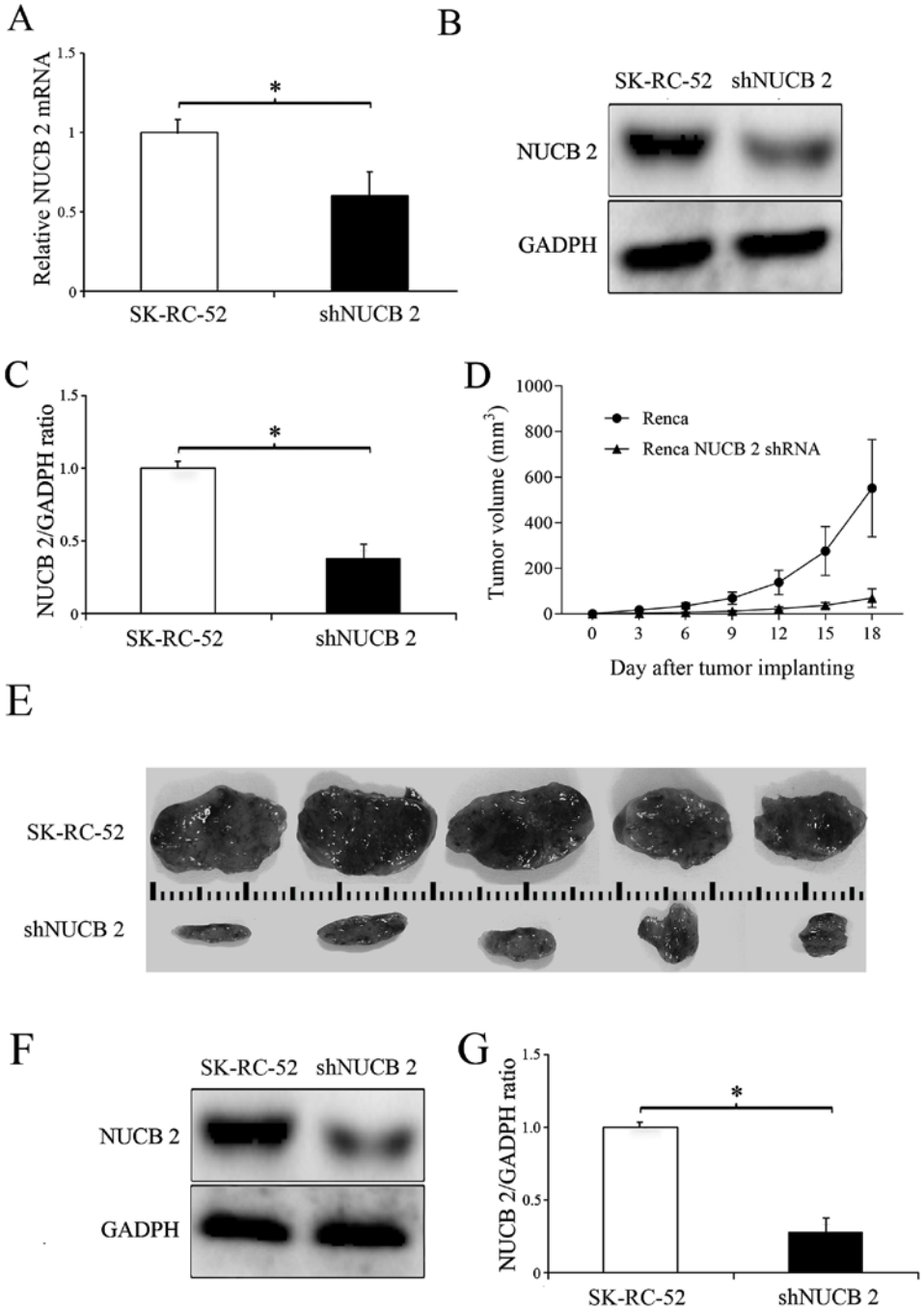

Figure 8. Suppression of NUCB-2 *in vivo* inhibits tumor formation in a renal cell carcinoma mouse model. (A) Relative mRNA levels of NUCB-2 normalized to those of GAPDH in shRNA or control cell lines. *P<0.05. (B) Protein expression levels of NUCB-2 in the shRNA and control cell lines. (C) Densitometry and statistical analysis of the western blots in the right panel. Relative protein levels of NUCB-2 normalized to those of GAPDH in samples. *P<0.05. (D) BALB/c mice were subcutaneously injected with Renca renal carcinoma cells in the rear flanks, and tumor size was measured every 2 days for the following 3 weeks. Growth of Renca cell tumors in a mouse model following the injection of an shRNA targeting NUCB-2 or a control injection. (E) *In vivo* tumors from mice implanted with the two different cell lines. (F) Relative protein expression levels of NUCB-2 normalized to those of GAPDH in shRNA or control cell lines at the end of the *in vivo* experiments. (G) Protein expression of NUCB-2 in the shRNA or control cell lines at the end of the *in vivo* experiment. *P<0.05. NUCB-2, nucleobindin 2; sh, short hairpin.

activating the mTOR signaling pathway, and ZEB1 activity was effectively inhibited when an mTOR inhibitor was used (51,52). Furthermore, the abrogation of AMPK expression by dorsomorphin restored NUCB-2-induced invasion, migration and the EMT in RCC in the NUCB-2-knockout SK-RC-52 cells. At the same time, the phosphorylation of two important downstream substrates of mTORC1, S6K and 4eBP1 was observed, suggesting their activation.

In addition, xenograft mouse experiments confirmed that the knockdown of NUCB-2 using a specific shRNA decreased renal cell tumor nodule formation compared with mice injected with cells expressing levels of high NUCB-2.

In conclusion, patient samples, cell lines and mouse models were analyzed, and NUCB-2 was identified as a valid marker associated with RCC malignant metastasis and a poor prognosis. The results of the present study suggest that NUCB-2 promotes

EMT in RCC via the AMPK/TORC1/ZEB1 pathway. These findings suggest that NUCB2 may serve as a potential diagnostic marker and therapeutic target for treating patients with RCC.

Acknowledgements

Not applicable.

Funding

This study was funded by the National Natural Science Foundation of China (Grant Nos. 81171996 and 81272289).

Availability of data and materials

The datasets used and/or analyzed during the current study are available from the corresponding author on reasonable request.

Authors' contributions

RT, WN, CZ and ZL conceived and designed the experiments. RT, WN, PD, YY and LC performed the experiments. SN collected and organized the experimental data. RT, XW and SL collected tissue samples, analyzed and interpreted the data and RT wrote the manuscript. CZ and ZL revised the manuscript. CZ and ZL revised and approved the final version of the manuscript. All authors read and approved the final manuscript.

Ethics approval and consent to participate

The present study was approved by The Ethical Committee of The First Affiliated Hospital of Jiamusi University (Jiamusi, China; approval no. HREC06FEB2016). In all cases, written informed consent was obtained, and the experiments were conducted in accordance with the Declaration of Helsinki.

Patient consent for publication

Not applicable.

Competing interests

The authors declare that they have no competing interests.

References

1. Pichler M, Hutterer GC, Chromecki TF, Jesche J, Kampel-Kettner K, Pummer K and Zigeuner R: Renal cell carcinoma stage migration in a single European centre over 25 years: Effects on 5- and 10-year metastasis-free survival. Int Urol Nephrol 44: 997-1004, 2012.
2. Siegel R, Ma J, Zou Z and Jemal A: Cancer statistics, 2014. CA Cancer J Clin 64: 9-29, 2014.
3. Parkin DM, Bray F, Ferlay J and Pisani P: Global cancer statistics, 2002. CA Cancer J Clin 55: 74-108, 2005.
4. Athar U and Gentile TC: Treatment options for metastatic renal cell carcinoma: A review. Can J Urol 15: 3954-3966, 2008.
5. Ljungberg B, Bensalah K, Canfield S, Dabestani S, Hofmann F, Hora M, Kuczyk MA, Lam T, Marconi L, Merseburger AS, *et al*: EAU guidelines on renal cell carcinoma: 2014 update. Eur Urol 67: 913-924, 2015.
6. Thiery JP: Epithelial-mesenchymal transitions in tumour progression. Nat Rev Cancer 2: 442-454, 2002.
7. Oh-I S, Shimizu H, Satoh T, Okada S, Adachi S, Inoue K, Eguchi H, Yamamoto M, Imaki T, Hashimoto K, *et al*: Identification of nesfatin-1 as a satiety molecule in the hypothalamus. Nature 443: 709-712, 2006.
8. Massari F, Ciccarese C, Santoni M, Brunelli M, Piva F, Modena A, Bimbatti D, Fantinel E, Santini D, Cheng L, *et al*: Metabolic alterations in renal cell carcinoma. Cancer Treat Rev 41: 767-776, 2015.
9. Zhang P, Sun Y and Ma L: ZEB1: At the crossroads of epithelial mesenchymal transition, metastasis and therapy resistance. Cell Cycle 14: 481-487, 2015.
10. Liu W, Huang YJ, Liu C, Yang YY, Liu H, Cui JG, Cheng Y, Gao F, Cai JM and Li BL: Inhibition of TBK1 attenuates radiation-induced epithelial-mesenchymal transition of A549 human lung cancer cells via activation of GSK-3β and repression of ZEB1. Lab Invest 94: 362-370, 2014.
11. Liu Z, Sun B, Qi L, Li H, Gao J and Leng X: Zinc finger E-box binding homeobox 1 promotes vasculogenic mimicry in colorectal cancer through induction of epithelial-to-mesenchymal transition. Cancer Sci 103: 813-820, 2012.
12. Li H, Song S, Xu Y, Zhao J and Liu H: Knockdown of ZEB1 suppresses the formation of vasculogenic mimicry in breast cancer cell line MDA-MB- 231 through downregulation of Flk-1. Minerva Med 108: 191-193, 2017.
13. Pavlides S, Tsirigos A, Migneco G, Whitaker-Menezes D, Chiavarina B, Flomenberg N, Frank PG, Casimiro MC, Wang C, Pestell RG, *et al*: The autophagic tumor stroma model of cancer: Role of oxidative stress and ketone production in fueling tumor cell metabolism. Cell Cycle 9: 3485-3505, 2010.
14. Martinez-Outschoorn UE, Balliet RM, Rivadeneira DB, Chiavarina B, Pavlides S, Wang C, Whitaker-Menezes D, Daumer KM, Lin Z, Witkiewicz AK, *et al*: Oxidative stress in cancer associated fibroblasts drives tumor-stroma co-evolution: A new paradigm for understanding tumor metabolism, the field effect and genomic instability in cancer cells. Cell Cycle 9: 3256-3276, 2010.
15. Kang J, Shakya A and Tantin D: Stem cells, stress, metabolism and cancer: A drama in two Octs. Trends Biochem Sci 34: 491-499, 2009.
16. Li QC, Wang HY, Chen X, Guan HZ and Jiang ZY: Fasting plasma levels of nesfatin-1 in patients with type 1 and type 2 diabetes mellitus and the nutrient-related fluctuation of nesfatin-1 level in normal humans. RegulPept 159: 72-77, 2010.
17. Gonzalez R, Reingold BK, Gao X, Gaidhu MP, Tsushima RG and Unniappan S: Nesfatin-1 exerts a direct, glucose-dependent insulinotropic action on mouse islet β-and MIN6 cells. J Endocrinol 208: R9-R16, 2011.
18. Suzuki S, Takagi K, Miki Y, Onodera Y, Akahira J, Ebata A, Ishida T, Watanabe M, Sasano H and Suzuki T: Nucleobindin 2 in human breast carcinoma as a potent prognostic factor. Cancer Sci 103: 136-143, 2012.
19. Cao X, Liu XM and Zhou LH: Recent progress in research on the distribution and function of NUCB-2/nesfatin-1 in peripheral tissues. Endocr J 60: 1021-1027, 2013.
20. Zhang H, Qi C, Wang A, Yao B, Li L, Wang Y and Xu Y: Prognostication of prostate cancer based on NUCB-2 protein assessment: NUCB-2 in prostate cancer. J Exp Clin Cancer Res 32: 77, 2013.
21. Zhang H, Qi C, Li L, Luo F and Xu Y: Clinical significance of NUCB-2 mRNA expression in prostate cancer. J Exp Clin Cancer Res 32: 56, 2013.
22. Zhang H, Qi C, Wang A, Li L and Xu Y: High expression of nucleobindin 2 mRNA: An independent prognostic factor for overall survival of patients with prostate cancer. Tumour Biol 35: 2025-2028, 2014.
23. Qi C, Ma H, Zhang HT, Gao JD and Xu Y: Nucleobindin 2 expression is an independent prognostic factor for clear cell renal cell carcinoma. Histopathology 66: 650-657, 2015.
24. Stengel A, Goebel M, Yakubov I, Wang L, Witcher D, Coskun T, Taché Y, Sachs G and Lambrecht NW: Identification and characterization of nesfatin-1 immunoreactivity in endocrine cell types of the rat gastric oxyntic mucosa. Endocrinology 150: 232-238, 2009.
25. William WN, Kim JS, Liu DD, Solis L, Behrens C, Lee JJ, Lippman SM, Kim ES and Hong WK and Lee HY: The impact of phosphorylated AMP-activated protein kinase expression on lung cancer survival. Ann Oncol 23: 78-85, 2012.
26. Zong H, Yin B, Zhou H, Cai D, Ma B and Xiang Y: Inhibition of mTOR pathway attenuates migration and invasion of gallbladder cancer via EMT inhibition. Mol Biol Rep 41: 4507-4512, 2014.

27. Lam JS, Klatte T and Breda A: Staging of renal cell carcinoma: Current concepts. Indian J Urol 25: 446-454, 2009.
28. Ebert T, Bander NH, Finstad CL, Ramsawak RD and Old LJ: Establishment and characterization of human renal cancer and normal kidney cell lines. Cancer Res 50: 5531-5536, 1990.
29. Gregersen I, Skjelland M, Holm S, Holven KB, Krogh-Sørensen K, Russell D, Askevold ET, Dahl CP, Ørn S, Gullestad L, *et al*: Increased systemic and local interleukin 9 levels in patients with carotid and coronary atherosclerosis. PLoS One 8: e72769, 2013.
30. Livak KJ and Schmittgen TD: Analysis of relative gene expression data using real-time quantitative PCR and the 2(-Delta Delta C(T)) method. Methods 25: 402-408, 2001.
31. Brodaczewska KK, Szczylik C, Fiedorowicz M, Porta C and Czarnecka AM: Choosing the right cell line for renal cell cancer research. Mol Cancer 15: 83, 2016.
32. Takeyama Y, Sato M, Horio M, Hase T, Yoshida K, Yokoyama T, Nakashima H, Hashimoto N, Sekido Y, Gazdar AF, *et al*: Knockdown of ZEB1, a master epithelial-to-mesenchymal transition (EMT) gene, suppresses anchorage-independent cell growth of lung cancer cells. Cancer Lett 296: 216-224, 2010.
33. Liu Y, El-Naggar S, Darling DS, Higashi Y and Dean DC: Zeb1 links epithelial-mesenchymal transition and cellular senescence. Development 135: 579-588, 2008.
34. Sánchez-Tilló E, Liu Y, de Barrios O, Siles L, Fanlo L, Cuatrecasas M, Darling DS, Dean DC, Castells A and Postigo A: EMT-activating transcription factors in cancer: Beyond EMT and tumor invasiveness. Cell Mol Life Sci 69: 3429-3456, 2012.
35. Xu Y, Pang XY, Dong M, Wen F and Zhang Y: Nesfatin-1 inhibits ovarian epithelial carcinoma cell proliferation in vitro. Biochem Biophys Res Commun 440: 467-472, 2013.
36. Yang ML, Zhang ZH, Wang C, Li K, Li SB, Boden G, Li L and Yang GY: Nesfatin-1 action in the brain increases insulin sensitivity through Akt/AMPK/TORC2 pathway in diet-induced insulin resistance. Diabetes 61: 1959-1968, 2012.
37. Li Z, Xu G, Li Y, Zhao J, Mulholland MW and Zhang W: mTOR-dependent modulation of gastric nesfatin-1/NUCB-2. Cell PhysiolBiochem 29: 493-500, 2012.
38. Saxton RA and Sabatini DM: mTOR signaling in growth, metabolism, and disease. Cell 9: 960-976, 2017.
39. Wullschleger S and Loewith R: TOR signaling in growth and metabolism. Cell 124: 471-484, 2006.
40. Laplante M and Sabatini DM: mTOR signaling in growth control and disease. Cell 149: 274-293, 2012.
41. Huang K and Fingar DC: Growing knowledge of the mTOR signalling network. Semin Cell Dev Biol 36: 79-90, 2014.
42. Ma XM and Blenis J: Molecular mechanisms of mTOR-mediated translational control. Nat Rev Mol Cell Biol 10: 307-318, 2009.
43. Viollet B, Horman S, Leclerc J, Lantier L, Foretz M, Billaud M, Giri S and Andreelli F: AMPK inhibition in health and disease. Crit Rev Biochem Mol Biol 45: 276-295, 2010.
44. Fu H, Zhu Y, Wang Y, Liu Z, Zhang J, Wang Z, Xie H, Dai B, Xu J and Ye D: High NUCB2 expression level represents an independent negative prognostic factor in Chinese cohorts of non-metastatic clear cell renal cell carcinoma patients. Oncotarget 15: 9188-9194, 2016.
45. Pinheiro C, Garcia EA, Morais-Santos F, Moreira MA, Almeida FM, Jubé LF, Queiroz GS, Paula ÉC, Andreoli MA, Villa LL, *et al*: Reprogramming energy metabolism and inducing angiogenesis: Co-expression of monocarboxylate transporters with VEGF family members in cervical adenocarcinomas. BMC Cancer 15: 835, 2015.
46. Saeidi N, Meoli L, Nestoridi E, Gupta NK, Kvas S, Kucharczyk J, Bonab AA, Fischman AJ, Yarmush ML and Stylopoulos N: Reprogramming of intestinal glucose metabolism and glycemic control in rats after gastric bypass. Science 341: 406-410, 2013.
47. Soga T: Cancer metabolism: Key players in metabolic reprogramming. Cancer Sci 104: 275-281, 2013.
48. Rattan R, Giri S, Singh AK and Singh I: 5-Aminoimidazole-4-carboxamide-1-beta-D-ribofuranoside inhibits cancer cell proliferation in vitro and in vivo via AMP-activated protein kinase. J Biol Chem 280: 39582-39593, 2005.
49. Dong D, Cai GY, Ning YC, Wang JC, Lv Y, Hong Q, Cui SY, Fu B, Guo YN and Chen XM: Alleviation of senescence and epithelial-mesenchymal transition in aging kidney by short-term caloric restriction and caloric restriction mimetics via modulation of AMPK/mTOR signaling. Oncotarget 8: 16109-16121, 2017.
50. Liu T, Sun Q, Li Q, Yang H, Zhang Y, Wang R, Lin X, Xiao D, Yuan Y, Chen L and Wang W: Dual PI3K/mTOR inhibitors, GSK2126458 and PKI-587, suppress tumor progression and increase radiosensitivity in nasopharyngeal carcinoma. Mol Cancer Ther 14: 429-439, 2015.
51. Kan JY, Yen MC, Wang JY, Wu DC, Chiu YJ, Ho YW and Kuo PL: Nesfatin-1/Nucleobindin-2 enhances cell migration, invasion, and EMT via LKB1/AMPK/TORC1/ZEB1 pathways in colon cancer. Oncotarget 7: 31336-31349, 2016.
52. Sun S, Hang T, Zhang B, Zhu L, Wu Y, Lv X, Huang Q and Yao H: miRNA-708 functions as a tumor suppressor in colorectal cancer by targeting ZEB1 through Akt/mTOR signaling pathway. Am J Transl Res 11: 5338-5356, 2019.